Vitrification and Devitrification of Rigid Amorphous Fraction of PET during Quasi-Isothermal Cooling and Heating

Huipeng Chen and Peggy Cebe*

Department of Physics and Astronomy, Tufts University, Medford, Massachusetts 02155

Received September 16, 2008; Revised Manuscript Received November 12, 2008

ABSTRACT: Poly(ethylene terephthalate), PET, was studied by quasi-isothermal (QI) temperature-modulated differential scanning calorimetry (TMDSC), in the limit of extremely slow scanning rates. For the first time, both the temperature-dependent crystalline fraction and rigid amorphous fraction (RAF) were quantitatively analyzed during quasi-isothermal cooling and reheating. Specific reversing heat capacity measurements show that most RAF vitrifies step by step during quasi-isothermal cooling after completion of crystallization. Upon subsequent QI reheating, the RAF devitrifies also step by step, and only a small RAF of 0.04 remains at 470 K, while melting starts above 473 K. To obtain the exact temperature of the start of melting, heat capacity measurements were made using subsequent standard DSC heating, after QI cooling. The temperature-dependent crystalline fraction was determined from Euler's equation. By combining this method with the QI results, the temperature-dependent phase fractions were obtained during standard DSC heating. We conclude that RAF completely devitrifies before the temperature reaches the crystal melting endotherm under the conditions used in this work. Therefore, bulk properties of PET that are dependent upon the fraction of the mobile amorphous phase will change within the temperature range from above T_g to the start of observable melting, even though the crystalline fraction is constant in this range.

Introduction

In semicrystalline polymers, the physical properties of the bulk depend upon the crystal and amorphous phase structure. The temperature-dependent mechanical, electrical, optical, solubility, and diffusion properties are highly sensitive to the temperature dependence of the liquidlike and solidlike fractions. The glass transition temperature (T_g) signifies the demarcation point. Well below T_g, all crystal and amorphous material is solidlike; from the start of the glass transition region to some temperature above it, the amorphous phase becomes liquidlike. The amount that becomes liquidlike and the temperature range over which the solid to liquid transition of the amorphous phase occurs are both critically important to understanding the bulk properties of semicrystalline polymers.

It is now recognized that semicrystalline polymers cannot be simply described by using a conventional two-phase model comprising crystalline and amorphous phases.[1−8] Wunderlich et al.[9,10] suggested that these two phases are connected by the tie molecules which will result in an interface due to the incomplete decoupling between the crystals and the amorphous chains, as a result of the imposed geometrical constraints. The interface, consisting of different molecular segments with different chain conformation, can appear with different properties from that of the bulk.

If the coupling is strong enough, Androsch and Wunderlich suggested that the affected molecular segments may be "sufficiently large, to produce a separate, intermediate phase with a glass transition separated from that of the unaffected amorphous phase".[10] The intermediate phase is called the "rigid amorphous fraction", RAF, and the conventional amorphous phase is called "mobile amorphous fraction", MAF. RAF was characterized by thermal analysis over 20 years ago by the deficit in the heat capacity increment at the glass transition of the MAF, since the RAF itself was assumed not to participate in the conventional glass transition process.[11,12] The size of the intermediate phase region associated with the RAF was estimated using X-ray and ^{1}H spin diffusion to be about 2−4 nm.[4,13] Later RAF was characterized by its impact on the gas transport properties of PET.[14]

Generally, the mobility of RAF is lower than that of MAF but higher than the mobility of the crystalline phase. So, in many polymers such as poly(ether ether ketone), PEEK,[1] poly(phenylene sulfide), PPS,[2] nylon-6,[8] and nylon-6,6,[15] the RAF will lose its solid character at a temperature above the conventional glass transition temperature, but below the completion of melting. An exception to this was found in poly(phenylene oxide), PPO, whose RAF was shown to devitrify above the melting temperature of the PPO crystals.[5]

Because RAF makes its own contribution to the bulk properties of polymers, the presence of RAF might result in a different temperature dependence of bulk properties of polymers compared to that expected from the simple two-phase model. Because of the distinct properties of RAF, studies have been performed on the kinetics of the vitrification and devitrification of RAF.[3,6−8,15] For poly(3-hydroxybutyrate), PHB, poly(carbonate), PC,[6,7] and isotactic polystyrene, iPS,[3] the RAF vitrified at the crystallization temperature. On the other hand, for nylon-6[8] and syndiotactic polypropylene,[6] a portion of the RAF vitrified after crystallization was completed. Regarding the devitrification process, in PHB and PC, the RAF was observed to become devitrified simultaneously with melting, and for nylon-6,6, the RAF devitrified before the start of melting.[6,7,15] Recently, Dargent et al. observed that the fragility parameter changes progressively during heating from above the glass transition of the MAF to the start of melting, which was thought to be due to the devitrification of RAF without any change of the crystallinity.[16]

If RAF devitrifies only with the melting of crystals, then in a wide temperature range from above T_g to the start of melting, it is safe to characterize the bulk properties without consideration of the change of RAF. Otherwise, RAF should be characterized at each temperature, in both heating and cooling, to help us understand the temperature dependence of the bulk properties. For this reason it is very important to understand the vitrification and devitrification of RAF in order to analyze the bulk properties

* Corresponding author: Tel 617-627-3365, Fax 617-627-3744, e-mail peggy.cebe@tufts.edu.

10.1021/ma802104a CCC: $40.75
Published on Web 12/05/2008

of polymers over a wide temperature range. Therefore, it is of great importance to characterize the RAF devitrification process at different temperatures rather than simply at a given temperature. However, quantitative analysis of RAF over a wide temperature range is still an open field.

Because of the practical importance of PET, there have been several studies of the rigid amorphous fraction in PET. Wunderlich and co-workers performed quasi-isothermal (QI) reheating on a slowly cooled sample of PET (having 44% crystallinity) and also QI cooling from the melt.[17,18] They suggested that RAF might vitrify after the completion of crystallization and devitrify before the start of melting. In this study, no quantitative analysis of RAF over a wide temperature range was done, and the crystallinity was unknown at temperatures above the glass transition temperature.[17,18] A different opinion about RAF devitrification was expressed by Schick et al.[19] Schick concluded that since no separate glass transition for RAF was detected before melting of crystals from DSC, and no significant differences of relaxation strength of dielectric and dynamic mechanical spectroscopy were observed for differently crystallized PET samples, then devitrification of RAF was deemed not to occur before the start of melting.[19] Righetti et al.[20] studied the kinetics of RAF by using standard DSC, but without measurement of crystallinity, and suggested that the vitrification of RAF started after the completion of primary crystallization and during secondary crystallization.

To resolve the controversy in the interpretation of the vitrification and devitrification of RAF in PET, we have combined standard and QI DSC techniques to provide a powerful tool *quantitatively* to assess both the temperature-dependent crystalline fraction and the rigid amorphous fractions. We perform quasi-isothermal cooling and heating to determine when the RAF vitrifies during cooling and when it devitrifies during reheating. We are addressing here the important issue about whether it is necessary for the temperature to be within the crystal melting endotherm in order for the rigid amorphous fraction to devitrify. Our heat capacity measurements show most RAF vitrifies step by step during the QI cooling *after* completion of crystallization. Upon subsequent QI heating, RAF devitrifies also step by step, and only a small RAF of 0.04 remains at 470 K, while melting starts above 473 K. Heat capacity measurements were also made using subsequent standard DSC heating, after QI cooling. The temperature-dependent crystalline fraction was determined from Euler's equation. By combining this method with the QI results, the temperature-dependent phase fractions were obtained during standard DSC heating. We conclude that under the conditions used in this work RAF devitrifies before the temperature reaches the crystal melting endotherm.

Experimental Section

Materials. The PET films were obtained from the former Allied Signal Corp. with intrinsic viscosity of 0.92 dL/g, measured in 60/40 phenol/trichloroethylene solution, giving a molecular weight of 25 000 g/mol calculated from the Mark−Houwink equation with $a = 0.640$ and $K = 14 \times 10^{-4}$ dL/g.

Thermal Measurements. The calorimetric analysis was carried out with a TA Instruments temperature-modulated DSC (TA Q100). Cooling was accomplished with a refrigerated cooling system (cooling capacity to 280 K). Dry nitrogen gas (grade 5.0) was purged into the DSC cell with a flow rate of 50 mL/min. Using indium reference, temperature calibration was done in the standard mode DSC (at 5 K/min) and in quasi-isothermal TMDSC mode (with an amplitude of 0.5 K and period of 60 s) immediately after calibration in the standard mode. The DSC Tzero* calibration and DSC heat capacity calibration suggested by TA Instruments were applied. We found that the QI experiments led to shift in the indium melting temperature of 0.1 K. To correct the temperatures from the QI measurements, we added a constant 0.1 K to the average temperatures. The heat capacity of sapphire was measured by QI TMDSC cooling and heating using amplitude of 0.5 K and period of 60 s from 273 to 573 K with a temperature step of 5 K. The heat capacity measured by QI cooling and heating overlapped with each other, and the value of heat capacity matched well (within 2%) with sapphire data provided from TA Instruments taken originally from ref 21.

We used a slightly lighter reference Al pan for all measurements including the baseline measurement and sapphire measurement to make it easier to adjust for asymmetry of the system using eq 1.[22] The quasi-isothermal cooling and heating experiments were done with temperature modulation amplitude of 0.5 K and period of $p = 60$ s, and stepwise temperature increase or decrease of the base temperature by 2−5 K was used, depending on the sample response. We ignored the first 10 min, and only used the last 10 min of the 20 min QI run, for data collection to calculate the reversing heat capacity C_p from

$$C_p = [A_\Phi/A_T\omega]K' \tag{1}$$

where A_Φ is the amplitude of the modulated heat-flow rate, A_T is the amplitude of the temperature modulation with frequency ω ($\omega = 2\pi/p$), and K' represents the calibration factor at the given conditions of measurement.[22−24] Since true thermodynamic reversibility has not been established, the usual term "reversing" for C_p is used.

Standard DSC measurements were performed at a heating rate of 5 K/min. Three runs were taken to obtain the heat capacity of all samples.[3,4] The first run is empty Al sample pan vs empty Al reference pan to obtain baseline correction. The second run is sapphire standard vs empty Al reference pan to calibrate heat flow amplitude. The third run is sample vs empty reference pan. All the empty Al reference pans and sample pans were kept the same in weight. The sample mass was kept at about 5−6 mg. Endothermic heat flow is presented by downward deflection from the baseline in our scans.

To determine the crystallinity of the sample at a certain temperature, the sample was heated up at 5 K/min in standard DSC mode, immediately after the completion of the quasi-isothermal TMDSC at that temperature. The crystallinity ϕ_C can be obtained from

$$\phi_C = \Delta H(\text{meas})/\Delta H_f \tag{2}$$

where ΔH(meas) is the measured heat of fusion of the semicrystalline polymer and $\Delta H_f = 140$ J/g is the heat fusion of 100% crystalline PET.[25]

Results and Discussion

In Figure 1, heat capacity of PET during the quasi-isothermal studies is displayed by the open circles for cooling and filled circles for subsequent reheating. The solid lines represent the heat capacity for different solid fractions, ϕ_S, where $\phi_S = \phi_C + \phi_{RA} = 1 - \phi_{MA}$ (ϕ stands for "fraction" and subscripts C, RA, and MA stand for crystal, rigid amorphous, and mobile amorphous, respectively) in the region of above glass transition to the start of melt. Lines marked by solid fractions $\phi_S = 1$ and $\phi_S = 0$ represent the heat capacity baselines for the 100% solid, C_p^{solid}, and 100% liquid, C_p^{liquid}, which match very well with PET data reported in the ATHAS data bank to within an error of less than 2%.[25]

To measure the crystallinity that has developed at different temperatures during the QI cooling, additional testing was performed in which the sample was heated up to the melt immediately using standard DSC, after it had been cooled to a given temperature quasi-isothermally. To avoid possibility of polymer degradation during the long QI treatments, a fresh sample was often used. The crystalline fraction ϕ_C was determined using eq 2. Our results in Figure 2a−e show that

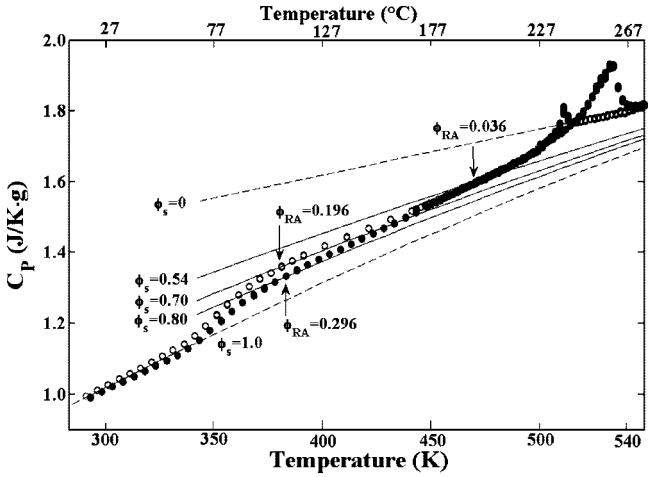

Figure 1. Heat capacity of PET during (a) QI cooling (open circles) and (b) subsequent QI reheating (filled circles). Dashed lines for $\phi_S = 0$ and $\phi_S = 1$ taken from ATHAS data bank.[25] The lines represent extrapolated heat capacity baselines determined from $\phi_S C_p^{solid}(T) + \phi_{MA} C_p^{liquid}(T)$, with the solid fractions, ϕ_S, as indicated. The third digits in the ϕ_{RA} are not significant ones but are included to show the range. Error on the phase fractions is ±2%.

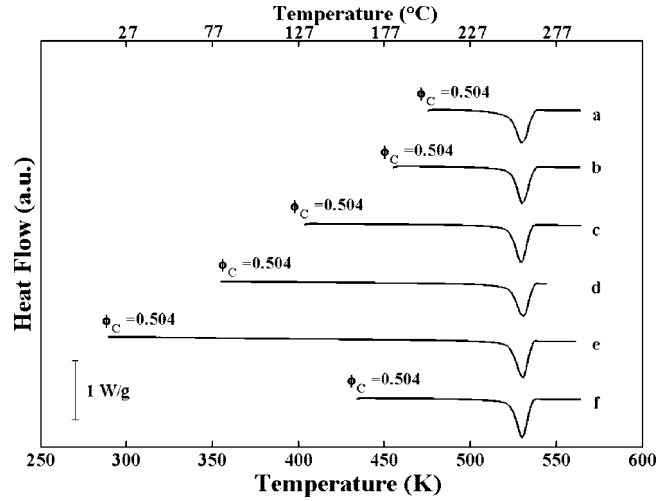

Figure 2. Heat flow vs temperature of PET heated at 5 K/min after QI cooling to (a) 473, (b) 453, (c) 401, (d) 351, and (e) 291 K and (f) PET after QI cooling and subsequent QI heating to 431 K. Samples (a)−(e) were cooled to the indicated temperatures quasi-isothermally and then immediately reheated, and the endotherm was recorded. Sample (f) was cooled quasi-isothermally to 291 K, then QI heated to 431 K, and finally scanned at 5 K/min to melt. Crystal fractions are indicated. The third digits in the ϕ_c are not significant ones but are included to show the range. Error on the crystal fraction is ±2%.

when the temperature was equal to or less than 473 K during the QI cooling experiment, the subsequent endothermic heat flow responses during reheating of the PET were identical. The crystalline fraction, ϕ_C, attained a value of 0.504, and thereafter as the temperature was further reduced, ϕ_C did not change. This important fact that ϕ_C did not change from 473 K down to room temperature means that we can determine ϕ_{MA} and ϕ_{RA} in the region from just above the glass transition up to the start of melting by using

$$C_p^{exp}(T) = \phi_S C_p^{solid}(T) + \phi_{MA} C_p^{liquid}(T) \quad (3a)$$

$$= (1 - \phi_{MA}) C_p^{solid}(T) + \phi_{MA} C_p^{liquid}(T) \quad (3b)$$

$$= (\phi_C + \phi_{RA}) C_p^{solid}(T) + (1 - \phi_C - \phi_{RA}) C_p^{liquid}(T) \quad (3c)$$

where C_p^{exp} is the experimentally measured heat capacity.

Results for ϕ_{RA} are shown in Figure 3. Φ_{RA} is very small at 473 K, only 0.036 (with ±2% error on phase fraction measurement), by which point the crystallization has been completed. During QI cooling from 473 K to 381 K, RAF increases to 0.196; thus, an additional 0.16 RAF was formed step by step during cooling, an amount that is 4 times greater than the RAF formed at higher temperatures, above 473 K. Somewhat below 381 K, the rubbery-to-glass transition occurs and during the glass transition, mobile amorphous chains now become vitrified. During the completion of the glass transition process upon cooling, all material reverts to the solid state, no matter whether it was originally crystalline, mobile, or rigid amorphous. All three phases have the same heat capacity in the solid state below T_g. Therefore, it is impossible from heat capacity measurements to distinguish RAF and MAF during the glass transition process or indeed at any temperature lower than T_g.

After QI cooling, the sample was reheated also by the QI method, which data are displayed by the filled circles in Figure 1. Since all the crystallization has been completed at 473 K during the previous cooling, it is reasonable to assume that ϕ_C remains unchanged below 473 K upon reheating. As a check on this assumption, one sample was QI cooled and then QI reheated to 431 K, at which point it was immediately heated at

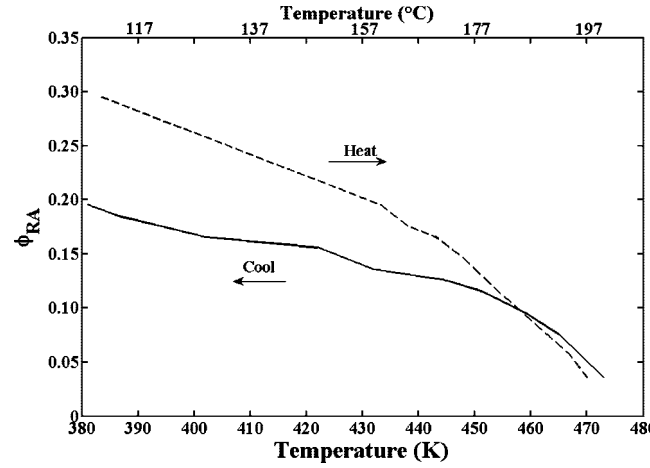

Figure 3. Rigid amorphous fraction, ϕ_{RA}, vs temperature during QI cooling (solid line) and subsequent QI reheating (dashed line) of PET.

5 K/min to melt it. The DSC trace of the 5 K/min scan is shown as curve f in Figure 2. The ϕ_C value determined from eq 2 is 0.504, the same as it was upon cooling, and again the error on phase fraction measurements is ±2%. The rigid amorphous fraction, ϕ_{RA}, can then be determined by eq 3c in the region from just above the glass transition up to the start of melting, in the temperature range from 473 to 383 K, where the glass transition process has already completed and all the MAF has attained the liquid heat capacity. On reheating to 383 K, ϕ_{RA} is 0.296, which is 0.10 *greater than* that it was at 381 K during QI cooling. This means about 0.10 of PET rigid amorphous fraction was formed during QI cooling and then reheating, within the temperature range 381−295 K. Wunderlich et al. also observed such a mismatch in heat capacity during the glass transition region upon reheating, compared to prior cooling.[17,18] This result could be due to the continuous vitrification of RAF during QI cooling within the glass transition region, in a process similar to physical aging. Struik suggested that the aging behavior of semicrystalline polymers could be explained by using a model of a glass transition extended toward the high-

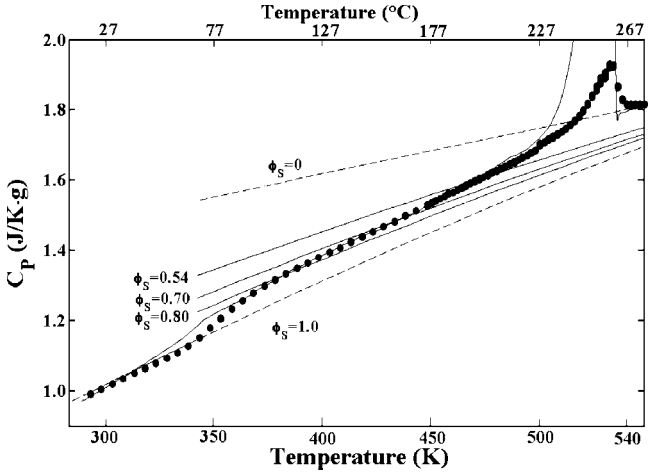

Figure 4. Heat capacity of PET from QI heating (filled circles) and standard heating (solid line) after QI cooling. Dashed lines for $\phi_S = 0$ and $\phi_S = 1$ taken from ATHAS data bank.[25]

temperature side.[26,27] During physical aging, Struik said the properties of the polymer will change with time by the slow and gradual approach to its thermodynamic equilibrium state, and materials become vitrified and progressively more brittle.[26,27] Comparing ϕ_{RA} at 383 K on heating with that ϕ_{RA} at 463 K on cooling, we observe that altogether more than 0.23 RAF was formed *after crystallization*. In Figure 1, during QI heating from 383 to 473 K (filled circles), the RAF starts to devitrify step by step and is almost totally devitrified at 470 K (only about 0.04 RAF is left) while melting starts above 473 K.

In Figure 4, standard DSC (solid line) is compared to QI reheating (filled circles), both taken after QI cooling treatment, such as that shown in Figure 1 (empty circles). Heat capacity from QI and standard heating overlapped well from 368 to 473 K, which provides strong support for the assumption that at 473 K crystal melting has not yet started. In Schawe's work on PET,[28] the occurrence of reversing melting at a temperature just above T_g was due to the low formation temperature of crystals, which were crystallized by cold crystallization at temperatures also just above T_g. The very low crystallization temperature will result in a low onset for the melting temperature. In our work, since all the crystals were formed at temperatures above 473 K, it is reasonable to assume here that neither reversing nor nonreversing melting of crystals occurs at temperatures below 473 K.

To calculate the change of crystallinity with temperature during standard heating after QI cooling, we used Euler's equation, which is based on a two-phase model including crystalline phase and amorphous phase:[3,29,30]

$$C_p^{\exp}(T) = \phi_C C_p^{\text{solid}}(T) + (1 - \phi_C) C_p^{\text{liquid}}(T) - (d\phi_C/dT)\Delta H_f(T) \quad (4)$$

where $C_p^{\exp}(T)$ is the experimentally measured specific heat capacity, ϕ_C is the temperature-dependent crystallinity, and $\Delta H_f(T)$ is the temperature-dependent heat of fusion corrected for undercooling by the factor $f = 2T/(T + T_m^0)$[3,29,30] using 553 K as the infinite crystal melting point, T_m^0.

The results of Euler analysis are presented in Figure 5. At about 480 K ϕ_C starts to decrease continuously with temperature increase. However, during heating at lower temperature from 400 to 480 K, ϕ_C appears (unreasonably) to increase slowly by a small amount. As shown above, the rigid amorphous fraction exists in PET during heating from 400 to 470 K, and this means a two-phase model is not correct for PET in this temperature

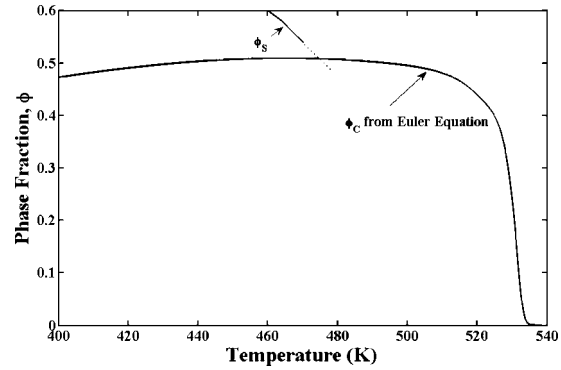

Figure 5. PET crystalline fraction, ϕ_C, calculated using Euler's equation (eq 4) based on a two-phase model. Solid fraction, ϕ_S (solid line), is calculated by eq 3a. ϕ_S (dotted line) is derived by linear extrapolation. The point of intersection of the extrapolated solid fraction and the crystalline fraction occurs at $T = 473.6$ K where $\phi_{RA} = 0$.

range. Since crystallization was finished during QI cooling by the time 473 K was reached, and there was no latent heat observed from 400 to 480 K when heat capacity from QI heating and standard heating were overlapped, we conclude the apparent increase in ϕ_C is a results of the limitation of using a two-phase assumption in the Euler equation.

Above 470 K, only about 0.04 RAF remains in PET. With continuous heating, the RAF should totally devitrify at a certain temperature where the three-phase model changes over to a two-phase model. We evaluate the solid fraction, $\phi_S = \phi_{RA} + \phi_C$, and show the temperature dependence of ϕ_S in Figure 5 (short solid line). ϕ_S is larger than ϕ_C for three-phase model ($\phi_{RA} > 0$) and equal to ϕ_C for two-phase model ($\phi_{RA} = 0$). In Figure 5, the intersection of the ϕ_S and ϕ_C curves signifies the point where the three-phase model changes over to a two-phase model. To locate this intersection point, we make the assumption that RAF continuously devitrifies during heating. By linear extrapolation, the ϕ_S dotted line is derived. We find that 473.6 K is the intersection temperature where RAF totally devitrifies, and the three-phase model changes to a two-phase model. Therefore, above 473.6 K the crystalline fraction can be determined by using Euler's equation. Below 473.6 K, ϕ_C is constant as demonstrated by the overlapping of the heat capacity from QI heating and from standard heating. Since crystallization has completed at 473 K during QI cooling, we may reasonably assert that the melting of PET crystals should start above 473 K. Then ϕ_{MA} also can be determined by $1 - \phi_{RA} - \phi_C$, and the results of the temperature dependence of the phase fractions, in the temperature region from above the glass transition to the completion of melting, are displayed in Figure 6. During subsequent standard DSC heating after QI heating, RAF devitrifies continuously and totally disappears at the start of crystal melting in PET. The vertical line marks the separation between the three-phase region and the two-phase region.

For PET, most of the RAF did not vitrify during crystallization in the quasi-isothermal cooling process. Possibly there is sufficiently high mobility of polymer chains within the amorphous region at these high temperatures, to allow crystals to form without simultaneous formation of most of the RAF. By subsequent QI cooling after the completion of crystallization, the mobility of polymer chains decreases step by step, more and more chains were confined, and RAF vitrified also step by step at different temperatures. The layer of amorphous chains next to the crystalline lamellae might be confined first, and subsequent layers may become immobilized as temperature decreases. Our result also demonstrates that secondary crystallization processes need not be associated with RAF formation, which contrasts with the suggestion of Righetti et al.[20] that RAF in PET might vitrify during secondary crystallization.

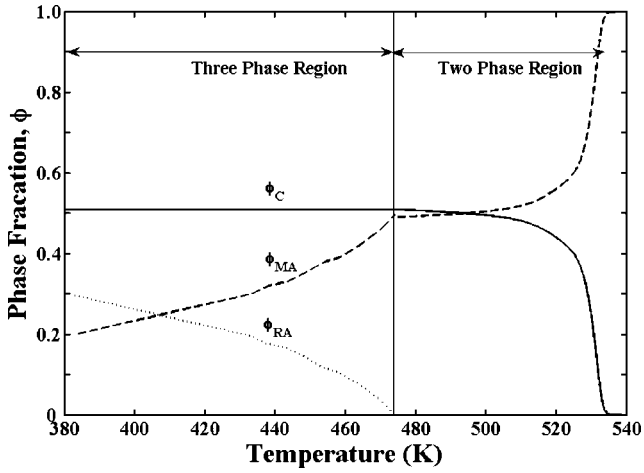

Figure 6. Temperature-dependent phase fractions of PET, for crystalline (solid line), mobile amorphous (dashed line), and rigid amorphous (dotted line) phases, during standard heating. The vertical line marks the separation between three-phase and two-phase regions.

Concerning the devitrification of RAF during reheating, our results show that by subsequent QI heating the mobility of the confined chains increases step by step with an increase of temperature, and the RAF devitrifies step by step. The layer farthest away from the crystalline region would be the most likely to relax first. At a temperature just before the start of crystal melting, the mobility of most chains was sufficiently high to eliminate confinement, and almost no RAF was left at this temperature.

In Schick's work,[19] the RAF (determined from DSC and TMDSC heat capacity) showed no separate glass transition step. Schick concluded that the crystals had to melt first, before the RAF could devitrify. Our results suggest that RAF can devitrify before the start of observable melting in PET (i.e., before the temperature reaches the crystal melting endotherm) at least during conditions of QI heating. Under these conditions, the devitrification of RAF seems to occur without presenting a traditional glass transition step in the heat capacity.

Conclusions

For the first time, the temperature-dependent RAF and crystalline fraction were both quantitatively analyzed during quasi-isothermal cooling and heating. For PET, most of the RAF vitrified after the completion of crystallization in a step by step manner during the QI cooling. Upon subsequent QI reheating, the RAF devitrifies also step by step and only a small RAF of 0.04 remains at 470 K, while melting starts above 473 K. To obtain the exact temperature of the start of melting, we made heat capacity measurements using subsequent standard DSC heating, after QI cooling. For PET, the vitrification and devitrification behavior of RAF during QI cooling and heating may be due to temperature-dependent changes of chain mobility of the mobile amorphous fraction out of which the RAF is formed. Furthermore, it should be realized that bulk properties of PET that are dependent upon the fraction of the mobile amorphous phase will change within the temperature range from above T_g to the start of observable melting, even though the crystalline fraction is constant in this range.

Acknowledgment. The authors acknowledge support from the National Science Foundation, Polymers Program of the Division of Materials Research, through DMR-0602473and the MRI Program under DMR-0520655 for thermal analysis instrumentation.

References and Notes

(1) Huo, P. P.; Cebe, P. *Colloid Polym. Sci.* **1992**, *25*, 902.
(2) Lu, X.; Cebe, P. *Polymer* **1992**, *37*, 4857.
(3) Xu, H.; Cebe, P. *Macromolecules* **2004**, *37*, 2797.
(4) Chen, H. P.; Xu, H.; Cebe, P. *Polymer* **2007**, *48*, 6404.
(5) Pak, J.; Pyda, M.; Wunderlich, B. *Macromolecules* **2003**, *20036*, 495.
(6) Schick, C.; Wurm, A.; Mohammed, A. *Thermochim. Acta* **2003**, *396*, 119.
(7) Schick, C.; Wurm, A.; Mohammed, A. *Colloid Polym. Sci.* **2001**, *279*, 800.
(8) Chen, H.; Cebe, P. *J. Therm. Anal. Calorim.* **2007**, *89*, 417.
(9) Wunderlich, B.; Mehta, A. *J. Polym. Sci., Polym. Phys. Ed.* **1974**, *12*, 255.
(10) Androsch, R.; Wunderlich, B. *Polymer* **2005**, *46*, 12556.
(11) Menczel, J.; Wunderlich, B. *J. Polym. Sci., Polym. Lett.* **1981**, *19*, 261.
(12) Suzuki, H.; Grebowicz, J.; Wunderlich, B. *Br. Polym. J.* **1985**, *17*, 1.
(13) Cheng, J.; Fone, M.; Reddy, V. N.; Schwartz, K. B.; Fisher, H. P.; Wunderlich, B. *J. Polym. Sci., Part B: Polym. Phys.* **1994**, *32*, 2683.
(14) Lin, J.; Shenogin, S.; Nazarenko, S. *Polymer* **2002**, *43*, 4733.
(15) Qiu, W. L.; Habenschuss, A.; Wunderlich, B. *Polymer* **2007**, *48*, 1641.
(16) Arnoult, M.; Dargent, E.; Mano, J. F. *Polymer* **2007**, *48*, 1012.
(17) Wunderlich, B. *Prog. Polym. Sci.* **2003**, *28*, 383.
(18) Okazaki, I.; Wunderlich, B. *Macromolecules* **1997**, *30*, 1758.
(19) Schick, C.; Dobbertin, J.; Potter, M.; Dehne, H.; Hensel, A.; Wurm, A.; Ghoneim, A. M.; Weyer, S. *J. Therm. Anal.* **1997**, *49*, 499.
(20) Righetti, M. C.; Tombari, E.; Angiuli, M.; Di Lorenzo, M. L. *Thermochim. Acta* **2007**, *462*, 15.
(21) Ditmars, D. A.; Ishihara, S.; Chang, S. S.; Bernstein, G.; West, E. D. *J. Res. Natl. Bur. Stand.* **1982**, *87*, 159.
(22) Boller, A.; Okazaki, I.; Ishikiriyama, K.; Zhang, G.; Wunderlich, B. *J. Therm. Anal. Calorim.* **1997**, *49*, 1081.
(23) Pyda, M.; Boller, A.; Grebowicz, J.; Chuah, H.; Lebedev, V.; Wunerlich, B. *J. Polym. Sci., Polym. Phys. Ed.* **1998**, *36*, 2499.
(24) Ishikiriyama, K.; Wunderlich, B. *J. Therm. Anal. Calorim.* **1997**, *50*, 337.
(25) Pyda, M. ATHAS data bank, http://athas.prz.rzeszow.pl/, **2008**.
(26) Struik, L. C. E. *Polymer* **1987**, *28*, 1521.
(27) Struik, L. C. E. *Polymer* **1987**, *28*, 1534.
(28) Schawe, J. E. K.; Hohne, G. W. H. *J. Therm. Anal.* **1996**, *46*, 893.
(29) Di Lorenzo, M. L.; Pyda, M.; Wunderlich, B. *J. Polym Sci., Part B: Polym. Phys.* **2001**, *39*, 1594.
(30) Pyda, M.; Di Lorenzo, M. L.; Pak, J.; Kamasa, P.; Buzin, A.; Grebowicz, J.; Wunderlich, B. *J. Polym. Sci., Part B: Polym. Phys.* **2001**, *39*, 1565.

MA802104A